Computers and Geotechnics 69 (2015) 301–319

Contents lists available at ScienceDirect

Computers and Geotechnics

journal homepage: www.elsevier.com/locate/compgeo

Research Paper

A simplified method for impedance and foundation input motion of a foundation supported by pile groups and its application

Xuezhang Wen [a,1], Fangyuan Zhou [b,*], Nobuo Fukuwa [c], Hongping Zhu [b,2]

[a] College of Civil Engineering, Hunan University, Changsha, Hunan, PR China
[b] School of Civil Engineering and Mechanics, Huazhong University of Science and Technology, Wuhan, Hubei, PR China
[c] Graduate School of Environmental Studies, Nagoya University, Nagoya, Japan

ARTICLE INFO

Article history:
Received 29 August 2014
Received in revised form 6 June 2015
Accepted 8 June 2015
Available online 18 June 2015

Keywords:
Impedance
Foundation input motion
Neighboring piles
Single equivalent pile
Soil–structure interaction

ABSTRACT

A simplified method is developed to analyze the impedance and foundation input motion of foundations supported by pile groups. In the proposed method, neighboring piles are replaced by a single equivalent pile. This replacement process reduces the number of degrees of freedom as well as the required computer memory and calculation time. To validate the simplified method, the impedance and foundation input motion of a raft foundation and an embedded foundation supported by pile groups with rigid and pin-jointed conditions between the pile head and foundation are calculated using both a simplified method and a rigorous numerical method. The results show that the proposed simplified method for the impedance and foundation input motion analysis of a foundation with a large number of piles yields sufficient accuracy. The simplified method is also applied to estimate the dynamic response of an isolated structure with a foundation supported by 2203 cement–soil piles with consideration of the soil–structure interaction. The results show that the dynamic response of the structure can be precisely simulated using the simplified method.

1. Introduction

Pile groups are widely used as foundations for high-rise structures and offshore platforms. One of the primary characteristics of these groups is that they consist of numerous piles. Various methods have been proposed in recent decades for analyzing pile groups subjected to seismic excitation. The finite element method (FEM) and boundary element method [1–9] are the most accurate and powerful approaches for computing the dynamic characteristics of pile group foundations; however, the required programs are complicated and inconvenient for practical engineering [10–14]. Models that use boundary element and finite element methods for the soil and piles require a large amount of computer memory, which results in high computational costs. This disadvantage is further heightened if the number of piles reaches several thousand, such that the dynamic response of the pile groups cannot be calculated even with several micro-computers. Therefore, the development of a method that can reduce the number of degrees of freedom for the dynamic response analysis of pile groups is necessary.

Approximate procedures that allow for the achievement of a solution with increased efficiency have been proposed in recent decades to reduce the number of degrees of freedom of the pile groups. Dobry et al. [15] developed a simple analytical solution to compute the dynamic impedances of floating rigidly capped pile groups embedded in uniform soil with due consideration of the pile-soil-pile interaction. Using the dynamic interaction factor, the impedances of two individual piles were calculated with one equivalent pile. The predictions of the simple method for vertical and rocking oscillations were comparable with those from rigorous numerical solutions. Gazetas and Makris [16,17] found that the error caused by the dynamic interaction factor in the impedance calculation for floating rigidly capped pile groups increases with the pile length. Nozoe [18] proposed a simple quasi-dynamic method for computing the impedances of pile groups installed in a homogeneous surface stratum situated on rigid bedrock. In the work by Varun et al. [19–21], using the macro-element to analyze the soil-pile interaction, the characteristics of soil resistance mechanisms and corresponding complex spring functions were developed based on finite element simulations. This was accomplished by equating the stiffness matrix terms and/or the overall numerically computed response to the analytical expressions derived

* Corresponding author. Tel.: +86 13638637165.
E-mail addresses: wenxuezhang@sohu.com (X. Wen), fangyuanzhou@hust.edu.cn (F. Zhou), fukuwa@sharaku.nuac.nagoya-u.ac.jp (N. Fukuwa), zhuhongping630@hotmail.com (H. Zhu).
[1] Tel.: +86 13875874213.
[2] Tel.: +86 27 87542631.

http://dx.doi.org/10.1016/j.compgeo.2015.06.004
0266-352X/

using the proposed Winkler model. Through the macro-element model proposed by Varun et al., the analysis of the soil-pile interaction problem can be simplified. Asega et al. [22] and Nogami [23] determined analytical expressions for the soil stiffness for a group of piles using a plane-strain and Kelvin–Voigt models. However, the n-times characteristic equation must be computed during the calculation procedure, and computational difficulties arise for an increasing number of piles.

Previous researchers have either proposed simplified models to facilitate the analysis of the dynamic response of the soil-pile problem or primarily focused on the objective of aggregating the degrees of freedom of the piles to the node located at the pile head in the vertical direction to reduce the computer memory and calculation time requirements. In addition, few studies on simplified methods of foundation input motion can be found in the literature. A simplified method is proposed in this paper, in which the discretization of the piles in the vertical direction remains unchanged, and the adjacent piles are aggregated as one equivalent pile in the horizontal direction; thus, the number of degrees of freedom of the pile groups in the horizontal direction is significantly reduced. The proposed simplified method can be used to analyze both the impedance and the foundation input motion of the piles group embedded in uniform soil or non-uniform layered soils. In addition, the proposed simplified method can be easily extended to the case of pile-raft foundations and embedded foundations supported by piles. The computational accuracy of the proposed simplified method was verified with a rigorous method for a foundation supported by pile groups. Finally, the simplified method was applied to estimate the dynamic response of an isolated structure with a foundation supported by 2203 cement–soil piles with consideration of the soil–structure interaction. The simulation result of the dynamic response of the structure is compared with the recorded data. The comparison shows that the soil–structure interaction of a foundation supported by pile groups can be precisely simulated using the simplified method.

2. Analytical theory of the impedance and foundation input motion

Consistent with the concept of SASSI proposed by Lysmer et al. [24], the substructure method and the thin-layer method [25–27] combined with the finite element method are employed to calculate the impedance and foundation input motion. In this work, as shown in Fig. 1, the soil-foundation system is separated into three components, i.e., the free field, foundation, and excavated soil, using the concept of the substructure method. The dynamic response of the free field is obtained using the thin-layer method (see Appendix A) linear interpolation function is used to calculate the dynamic response of the nodes located between the two adjacent layered soil interfaces. At the same time, a paraxial boundary condition (see Appendix A) [28,29] is used to simulate the bottom boundary of the layered soil. The embedded foundation and the excavated soil of the embedded foundation are modeled using three-dimensional isoparametric solid elements, and beam elements are used to simulate the piles and the excavated soil of the piles. The Green's function solutions for a concentrated load and for a uniformly distributed load acting on a disk (when the excitation node and reception node coincide with each other) are applied to form the flexibility matrix of the soil-foundation system.

The analysis procedure in this paper is based on the following basic assumptions:

(1) The soil is assumed to be a homogeneous or layered viscoelastic medium;
(2) The foundation remains in close contact with the surrounding soil, no slippage is allowed at the soil-foundation interface;
(3) The foundation is assumed to be a massless rigid foundation (the mass of the foundation is considered in the superstructure using the substructure method).

2.1. Rigorous method

The equation of motion for the MRF (massless rigid foundation)-pile-soil system based on the structure method shown in Fig. 1 is (the calculation is performed in the frequency domain, and the term $e^{i\omega t}$ is omitted in the formula):

$$([K]^G + [S]^S - [S]^E)\{u\} = \{F\} \tag{1}$$

Where $[S] = [K] - \omega^2[M]$, and $[K], [M]$, $\{u\}$, and are the stiffness matrices, mass matrices, and displacement vector, respectively. The massless rigid foundation and pile as well as the free field and excavated soil are denoted by the superscripts S, G, and E, respectively. The embedded foundation is modeled by a solid element for the embedded foundation supported on the pile groups. The beam element is employed to form the stiffness matrices of the piles. The piles are treated as generalized beam with two nodes and 12 degrees of freedom; thus, a complete stiffness matrix is employed for the piles. A complete stiffness matrix is formed (1) so that the foundation input motion can be calculated and (2) to facilitate the extension of the method to piled-raft foundation and piles with an embedded foundation.

The stiffness matrix $[K]^G$ of the free field can be calculated with the following equation:

$$[K]^G = [G]^{-1} \tag{2}$$

In this equation, the Green's function solution for a concentrated load and for a uniformly distributed load acting on a disk (when the excitation node and reception node coincide with each other) is applied to form the flexibility matrix of the free field $[G]$ [27].

To calculate the impedance of the massless rigid foundation, the subscripts F and O are used to denote the degrees of freedom of the foundation and piles (except the head of the pile), respectively, as shown in Fig. 1(a). Thus, Formula (1) can be rewritten as

$$\begin{bmatrix} [S_{FF}] & [S_{FO}] \\ [S_{OF}] & [S_{OO}] \end{bmatrix} \begin{Bmatrix} \{u_F\} \\ \{u_O\} \end{Bmatrix} = \begin{Bmatrix} \{F_F\} \\ \{F_O\} \end{Bmatrix} \tag{3}$$

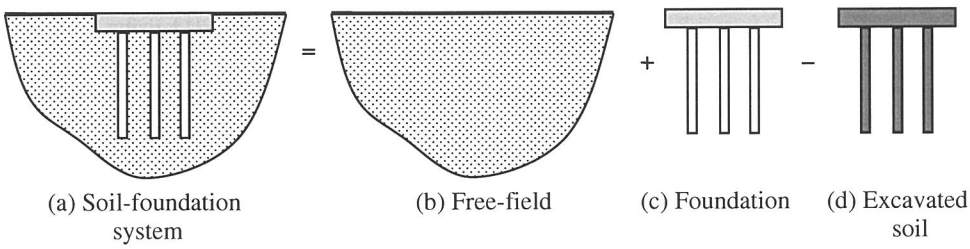

Fig. 1. Soil foundation model based on the substructure method.

Decomposition of Formula (3) yields

$$[S_{FF}]\{u_F\} + [S_{FO}]\{u_O\} = \{F_F\} \tag{4}$$

$$[S_{OF}]\{u_F\} + [S_{OO}]\{u_O\} = \{F_O\} \tag{5}$$

Using Formula (5), Formula (6) can be obtained as follows:

$$\{u_O\} = -[S_{OO}]^{-1}[S_{OF}]\{u_F\} + [S_{OO}]^{-1}\{F_O\} \tag{6}$$

Substituting Formula (6) into Formula (4) produces

$$([S_{FF}] - [S_{FO}][S_{OO}]^{-1}[S_{OF}])\{u_F\} = \{F_F\} - [S_{FO}][S_{OO}]^{-1}\{F_O\} \tag{7}$$

By converting Formula (7) to a motion equation with six degrees of freedom for the massless rigid foundation, the impedance of the foundation can be obtained as

$$[K_F] = [T]^T([S_{FF}] - [S_{FO}][S_{OO}]^{-1}[S_{OF}])[T] \tag{8}$$

where is the coordinate transformation matrix relative to the geometric center of the massless rigid foundation.

For the foundation input motion, the external force is

$$\begin{Bmatrix} \{F_F\} \\ \{F_O\} \end{Bmatrix} = [K]^G\{u\}_G = \begin{bmatrix} [K_{FF}]^G & [K_{FO}]^G \\ [K_{OF}]^G & [K_{OO}]^G \end{bmatrix} \begin{Bmatrix} \{u_F\}_G \\ \{u_O\}_G \end{Bmatrix} \tag{9}$$

where $\{u_F\}_G$ and $\{u_O\}_G$ denote the responses of the free field and the soil subjected to seismic wave excitation, respectively. The foundation input motion can be obtained by substituting Formula (9) with Formula (3).

The impedance and foundation input motion of a foundation can be computed based on the above procedure. A comparison of this procedure method with the solution of Kaynia & Kausel [30] for a group of 2 × 2 and 4 × 4 piles (shown in Fig. 2) in a homogeneous half-space as a function of the non-dimensional frequency, $a_0 = \omega d/V_s$ (where d is the pile diameter and V_s is the shear wave velocity of the soil), is portrayed in Figs. 3 and 4. For the horizontal case, the dynamic impedance was normalized with respect to the horizontal static stiffness of a single pile in the group, whereas for the vertical and rocking dynamic impedance, the vertical static stiffness of a single pile is used for normalization. For the results presented in this work, it has been assumed that v_s (Poisson ratio of the soil) = 0.4, $E_{pile}/E_{soil} = 100$ (E_{pile} and E_{soil} are the moduli of elasticity of the piles and soil, respectively), v_p (Poisson ratio of the piles) = 0.25, L (length of the piles) = 15 d (where d is the pile diameter), S (pile spacing) = 5d, and $\rho_s/\rho_p = 0.7$, where ρ_s and ρ_p are the mass densities of the soils and piles, respectively, with N identical piles in the group. As shown in Figs. 3 and 4, the predictions of the described procedure method compare well with the solution of Kaynia & Kausel [30]. The analysis method described in Section 2.1 can provide accurate results for the dynamic impedance and foundation input motion of the pile group.

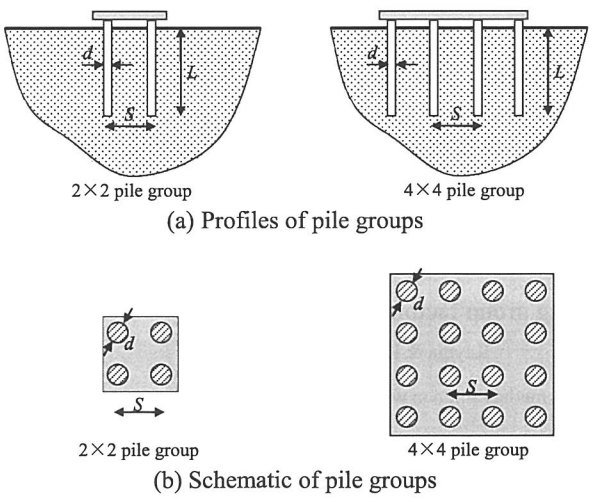

Fig. 2. Profiles and schematic of the pile groups.

However, Formula (8) demonstrates that an increase in the number of piles requires a large amount of computer memory to formulate and compute the matrix depicted in the equation; thus, the rigorous method has high computational requirements.

2.2. Simplified method

A simplified method that aggregates neighboring piles into a single equivalent pile (shown in Fig. 5) was developed to address the computational problems of the rigorous method. The single equivalent pile is referred to in this study as the *aggregated pile*. The *aggregated pile* is treated as a generalized beam with 2 nodes and 12 degrees of freedom. The proposed simplified method aims to maintain the impedance and foundation input motion of the pile groups before and after aggregation. The thin-layer method [25–27] was employed to compute the dynamic stiffness of the springs and dashpot connected between the pile and the surrounding soil. The weighted average of the pile displacement at the reception surface was employed to denote the displacement of the aggregated pile.

2.2.1. Cross-sectional parameters of the aggregated pile

As shown in Fig. 5, the cross-sectional parameters of the aggregated pile are the sum of the cross-sectional parameters of each pile in the pile group, as depicted in Formula (10).

$$A = \sum A_i \tag{10a}$$

$$A_1 = \sum A_{1i} \tag{10b}$$

$$A_2 = \sum A_{2i} \tag{10c}$$

$$I_{11} = \sum I_{11i} \tag{10d}$$

$$I_{22} = \sum I_{22i} \tag{10e}$$

$$J = \sum J_i \tag{10f}$$

$$X = \sum x_i A_i / \sum A_i \tag{11a}$$

$$Y = \sum y_i A_i / \sum A_i \tag{11b}$$

where A, A_1, A_2 represent the cross-sectional area, the effective shear area along the 1(x) axis, and the effective shear area along the 2(y) axis, respectively; I_{11}, I_{22} denote the moment of inertia of the cross-sectional area on the 1(x) axis and 2(y) axis, respectively; and J is the torsional moment of inertia in the cross-sectional area. The coordinate position of the aggregated pile is identified by Formula (11).

The rocking stiffness of a foundation with multiple aggregated piles (Fig. 6) was computed using the sum of the products of the dynamic stiffness of the aggregated piles in the vertical direction (z-axis) and the distance from the aggregated piles to the center of the foundation. For simplification, the self-rocking stiffness of the aggregated piles was ignored.

2.2.2. Thin-layer solution for the aggregated pile under seismic excitation

As shown in Fig. 7, S and R are the source surface at which the dynamic forces are applied and the reception surface, respectively, and F_j denotes the dynamic force applied on the j_{th} pile at source surface S. If the sum of the dynamic forces applied on the source surface is 1, then F_j can be depicted as in Formula (12).

$$F_j = \frac{w_j}{\sum_{k=1}^{N_s} w_k} \tag{12}$$

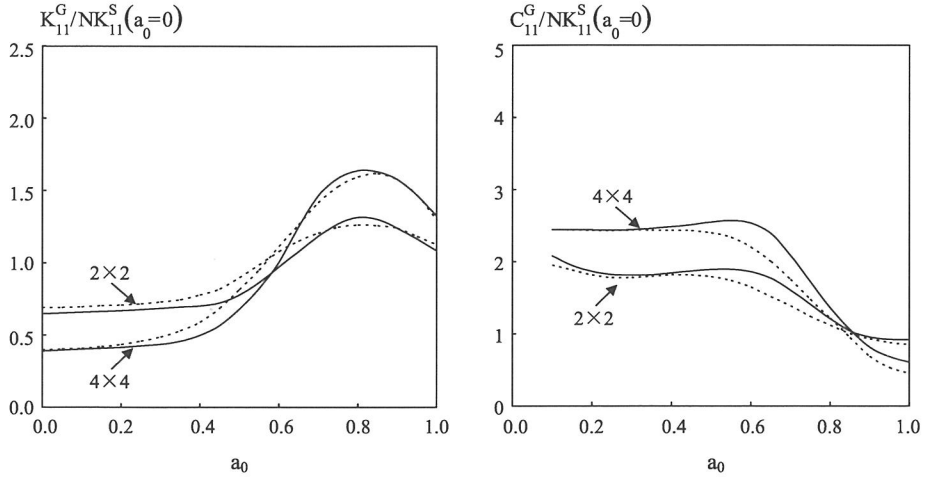

(a) Horizontal stiffness and damping group factors

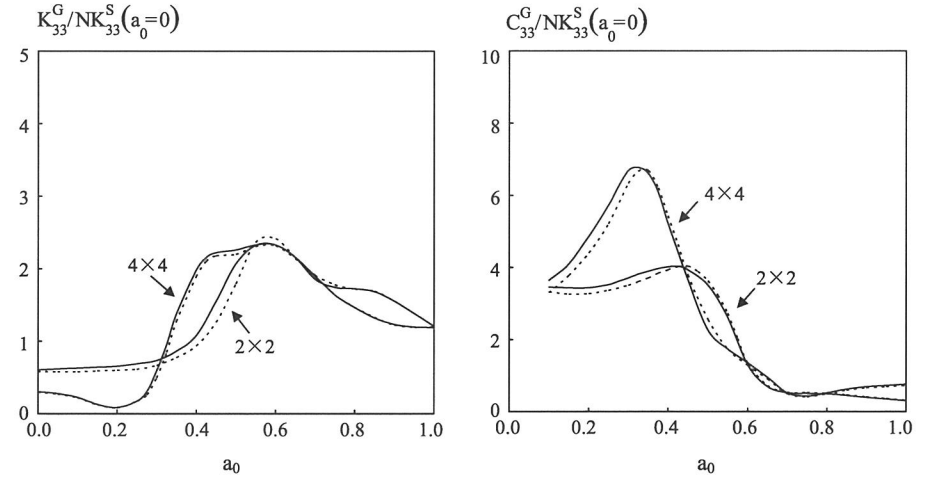

(b) Vertical stiffness and damping group factors

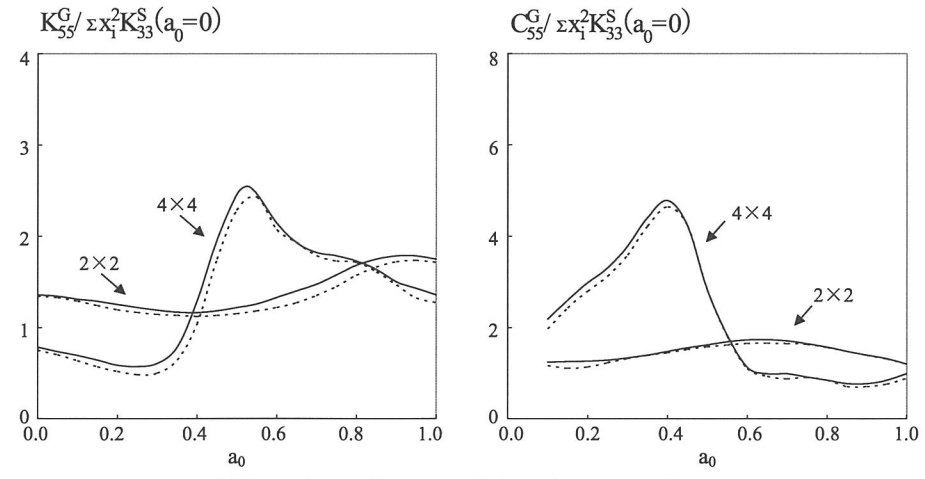

(c) Rocking stiffness and damping group factors

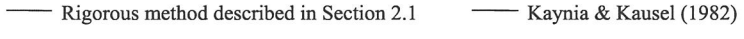

Fig. 3. Stiffness and damping group factors as a function of frequency: comparison of the rigorous method solution with the solution of Kaynia & Kausel [30] for a group of 2×2 and 4×4 piles in a homogeneous half-space.

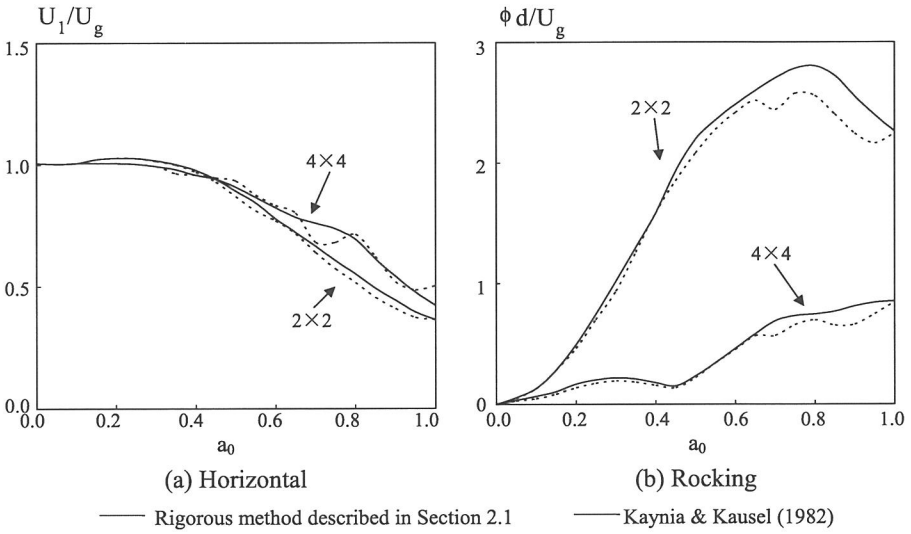

Fig. 4. Foundation input motion as a function of frequency: comparison of the rigorous method solution to the solution of Kaynia & Kausel [30] for a group of 2 × 2 and 4 × 4 piles in a homogeneous half-space.

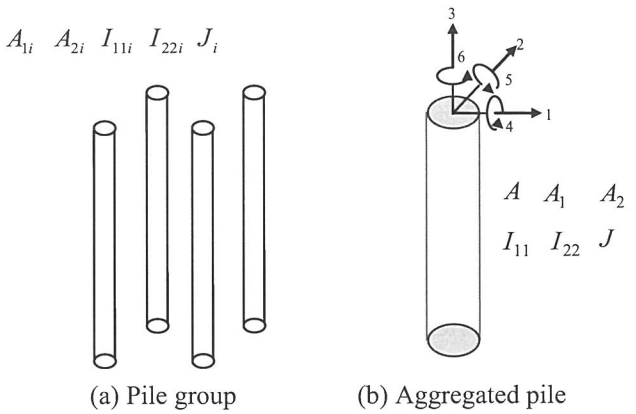

Fig. 5. Cross-sectional characteristics of the pile group and the aggregated pile.

where w_j represents the weight. If a non-unique diameter is used in the pile groups, the section area of the piles can be used as the weight, and N_S, N_R is the number of piles in the group. The displacement of the i_{th} pile at reception surface R caused by the force applied on the source surface can be depicted as in Formula (13).

$$u_{RSi} = \sum_{j=1}^{N_S} F_j u_{RSij} = \sum_{j=1}^{N_S} \left(\frac{w_{Sj}}{\sum_{k=1}^{NS} w_{Sk}} u_{RSij} \right) = \frac{\sum_{j=1}^{N_S} w_{Sj} u_{RSij}}{\sum_{k=1}^{N_S} w_{Sk}} \tag{13}$$

where u_{RSij} is the displacement of the i_{th} pile at reception surface R caused by force F_j applied on source surface S and u_{RSij} is computed with the thin-layer method. Thus, the weighted average of the displacement of the piles at the reception surface can be written as in Formula (14).

$$u_{RS} = \frac{\sum_{i=1}^{N_R} w_{Ri} u_{RSi}}{\sum_{i=1}^{N_R} w_{Ri}} = \frac{\sum_{i=1}^{N_R} \sum_{j=1}^{N_S} w_{Ri} w_{Sj} u_{RSij}}{\sum_{i=1}^{N_R} w_{Ri} \sum_{k=1}^{N_S} w_{Sk}} \tag{14}$$

If the cross-sectional area of the pile is used as the weight, the average for a pile group with a uniform pile diameter u_{RS} can be rewritten as

$$u_{RS} = \frac{\sum_{i=1}^{N_R} \sum_{j=1}^{N_S} u_{RSij}}{N_R N_S} \tag{15}$$

Neighboring piles can be replaced by an equivalent aggregated pile using the analysis procedure described in this section. The dynamic response of the aggregated pile can be obtained using Formula (15). Therefore, the problem of large pile groups is converted into the problem of solving for the dynamic response of the aggregated piles; in this way, the number of degrees of freedom of the pile groups is significantly reduced.

3. Investigation of the effectiveness of the simplified method

To validate the proposed simplified method, the impedance and the foundation input motion of a raft foundation and an embedded

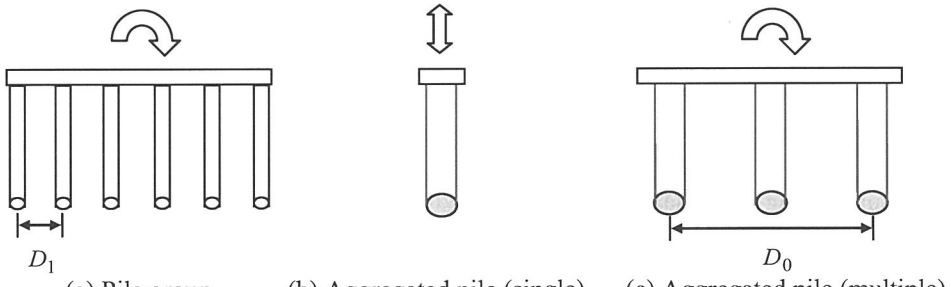

Fig. 6. Rocking stiffness of the pile group and the aggregated pile.

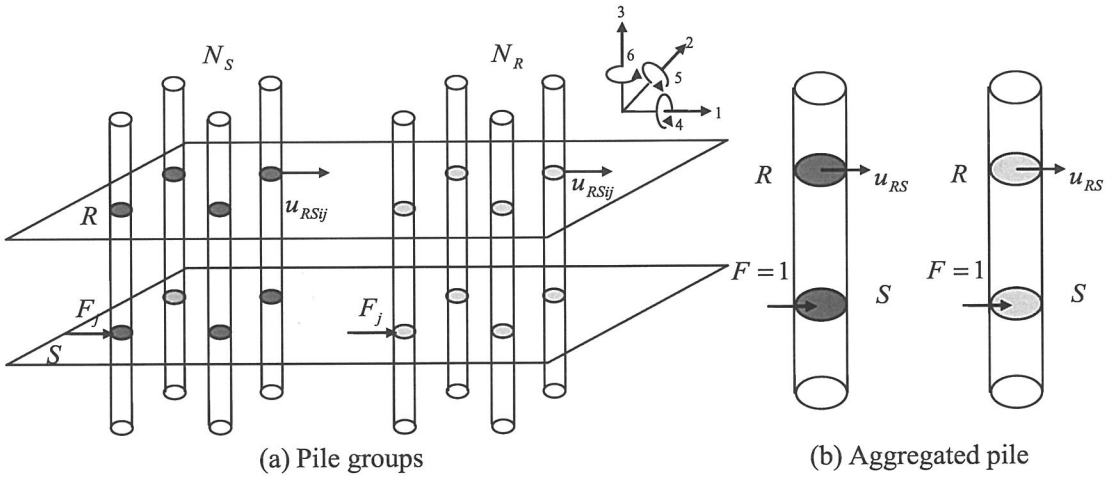

Fig. 7. Multi-point excitation.

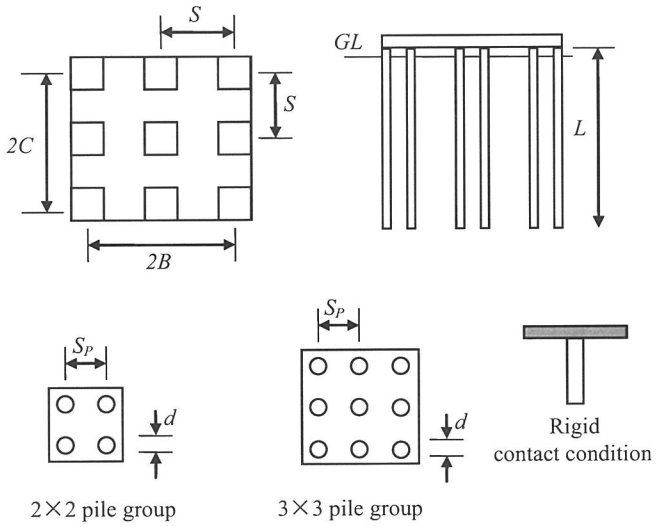

Fig. 8. Raft foundation supported by pile groups.

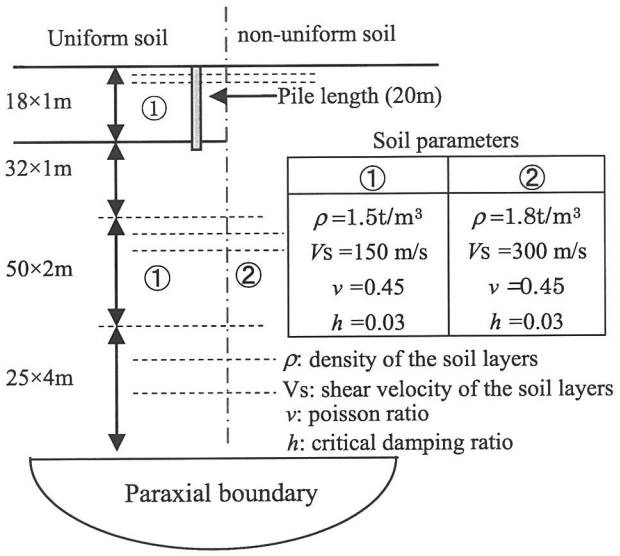

Fig. 9. Foundation conditions.

foundation supported by pile groups were calculated with the simplified and rigorous numerical methods.

3.1. Use of the simplified method for a foundation supported by pile groups with rigid contact conditions between the pile head and the foundation

The layout of a raft foundation supported by pile groups is shown in Fig. 8. The piles are 600 mm (d) in diameter with a length of 20 m (L). These piles were placed at a spacing of 2.5d (S_p). The spacing (S) between the centers of the two adjacent pile groups for the 2 × 2 and 3 × 3 pile groups is 9.75 m and 9.0 m, respectively. The dimensions of the raft foundation are 21 m × 21 m. The contact condition between the pile head and the foundation is rigid, which means that the freedom of the jointed point between the pile head and the bottom of the foundation is fixed; thus, the forces and moments can be transmitted freely, as shown in Fig. 8. The soil conditions surrounding the foundation are shown in Fig. 9. To ensure the accuracy of the thin layer method at low frequency, the relationship between the wavelength λ and the depth of the soil L should be $\lambda/L \leqslant 4$. Meanwhile, to ensure the accuracy of the thin layer method at high frequency, the relationship between the wavelength λ and the depth of the soil layer H should be $\lambda/H \geqslant 6$[31]. In this paper, the frequency domain of the excitation varies from 0.1 Hz to 10 Hz, thus, the soil profile shown in Fig. 9 is employed. The impedance and foundation input motion of the raft foundation supported by pile groups were investigated under uniform and non-uniform soil conditions, respectively. The normal incident *SH* wave from the bottom of the foundation was used as an excitation source. Fig. 10 shows the dynamic impedance and foundation input motion of raft foundations with 2 × 2 pile groups determined using the simplified and rigorous methods. The dynamic impedances are presented for the horizontal and rocking modes of vibration. The complex dynamic impedance ($k + ic$) is resolved into stiffness (real: k) and damping (imaginary: c) components, and the results for the 2 × 2 pile groups show notably good agreement. A minor difference was generated in the high-frequency domain. Fig. 11 shows the dynamic impedance and foundation input motion of raft foundations with 3 × 3 pile groups. The figure indicates that the results show notably good agreement in terms of the impedance and foundation input motion along the horizontal direction.

As shown in Figs. 10(b) and 11(b), in the low-frequency domain, the quasi-static stiffness in the rocking direction calculated from the simplified method is slightly smaller than that obtained with

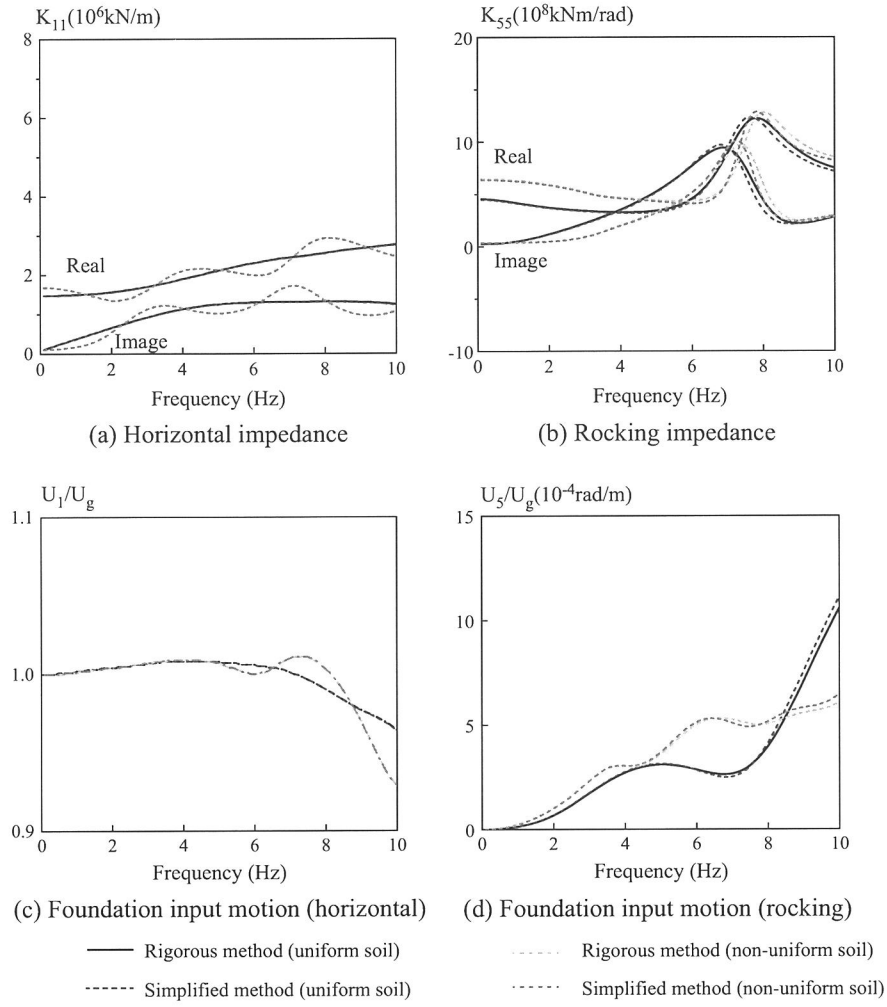

Fig. 10. Raft foundation supported by 2 × 2 pile groups. Comparison of current results with the rigorous method solution.

the rigorous method; the quasi-static stiffness for the 2 × 2 pile groups is 1.5% and that of the 3 × 3 pile groups is approximately 3.6%. However, a marked difference was generated for the rocking impedance in the high-frequency domain (see Fig. 11(b)). This is because most of the rocking stiffness originates from the vertical impedance of the piles. The rocking stiffness of a foundation with multiple aggregated piles was computed using the sum of the products of the dynamic stiffness of the aggregated piles in the vertical direction and the distance from the aggregated piles to the center of the foundation. Thus, the calculation accuracy of the vertical impedance of the pile groups determines the validity of the calculated rocking impedance. Fig. 12 show a comparison of the results obtained through the proposed simplified method with the rigorous method solution in the vertical direction for the raft foundation supported by 2 × 2 and 3 × 3 pile groups. Fig. 12 show that for the vertical impedance with increasing number of aggregated piles, a difference arises between the results of the proposed simplified method and the rigorous method solution in the high-frequency domain; hence, the calculation accuracy of the proposed simplified method will decrease in terms of the rocking stiffness with increasing number of aggregated piles. Fig. 12(a) shows that for 2 × 2 pile groups, the vertical impedance calculated using the proposed simplified method is almost identical to that of the rigorous method solution; thus, the rocking impedances obtained using the proposed simplified method and the rigorous method are similar to each other. However, Fig. 12(b) shows that for 3 × 3 pile groups (vertical impedance), a difference arises between the results of the proposed simplified method and the rigorous method solution in the high-frequency domain; thus, for the 3 × 3 pile groups, the rocking impedance obtained using the proposed simplified method is different than that of the rigorous method solution in the high-frequency domain. The aggregated pile represents the average effect of each pile in the group in the high-frequency domain, and because the ratio of the distance between the piles and the wavelength is large, the calculated Green's function exhibits a large discreteness. Therefore, the effect of calculating the impedance of 2 × 2 pile groups in the vertical direction is better that of 3 × 3 pile groups using the proposed simplified method.

The layout of an embedded foundation supported by pile groups is shown in Fig. 13. The embedded depth of the foundation (E) is 4.0 m, and the length of the pile (L) under the embedded foundation is 16 m. The other parameters shown in Fig. 13 are the same as those depicted in the case of the raft foundation. Fig. 14 shows the dynamic impedances and foundation input motions of the embedded foundation supported by 2 × 2 pile groups using the simplified and rigorous methods. As expected, Fig. 14 shows that the impedances and foundation input motions obtained from the simplified method are similar to those calculated using the rigorous method. Similar to the raft foundation supported by pile groups, a minor difference was generated in the high-frequency domain. Fig. 15 shows the dynamic impedance and foundation

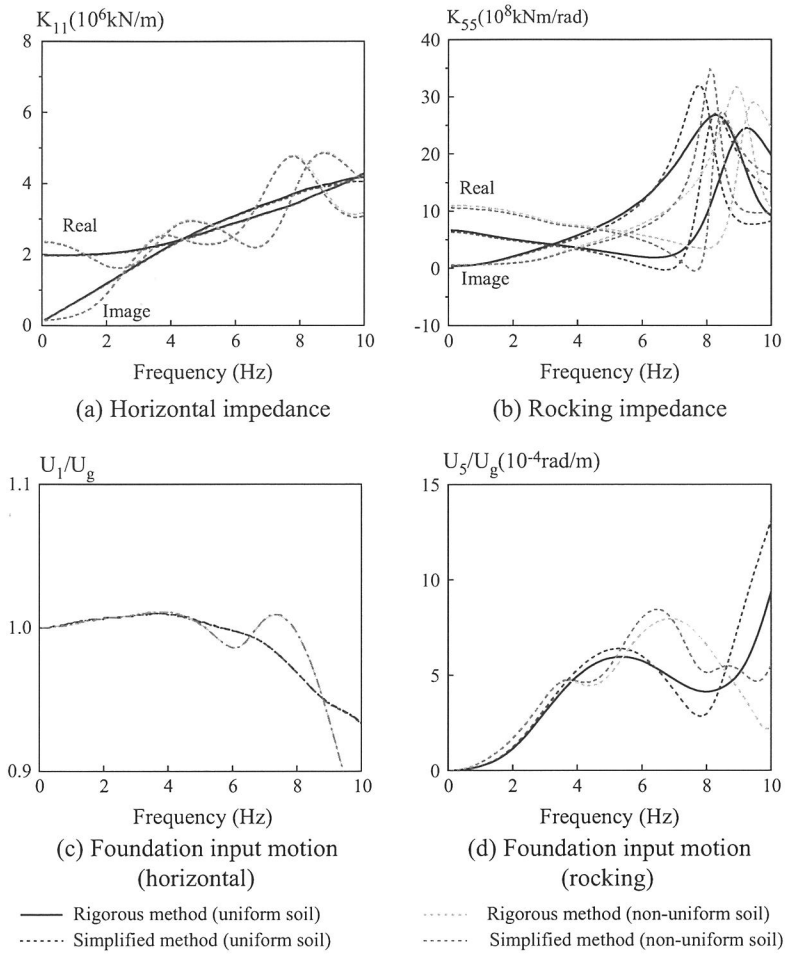

Fig. 11. Raft foundation supported by 3 × 3 pile groups. Comparison of current results with the rigorous method solution.

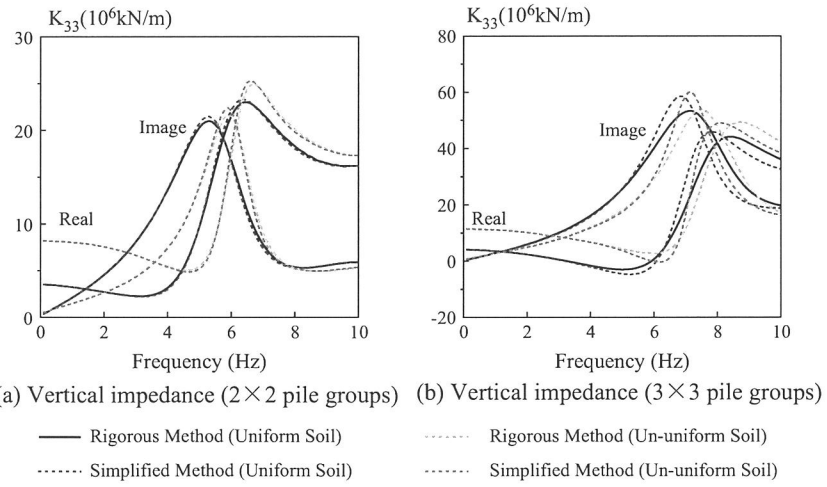

Fig. 12. Vertical impedances of the raft foundation with pile groups. Comparison of present results with rigorous method's solution.

input motion of the embedded foundation supported by 3 × 3 pile groups. Compared with the results depicted in Fig. 14, the difference between the simplified and rigorous method solutions for the rocking response in the high-frequency domain grows for an increasing number of piles in the group.

3.2. Use of the simplified method for a foundation supported by pin-jointed pile groups

The simplified method was used for raft and embedded foundations supported by pile groups with pin-jointed conditions (the rocking freedom of the jointed point is free, and hence, the

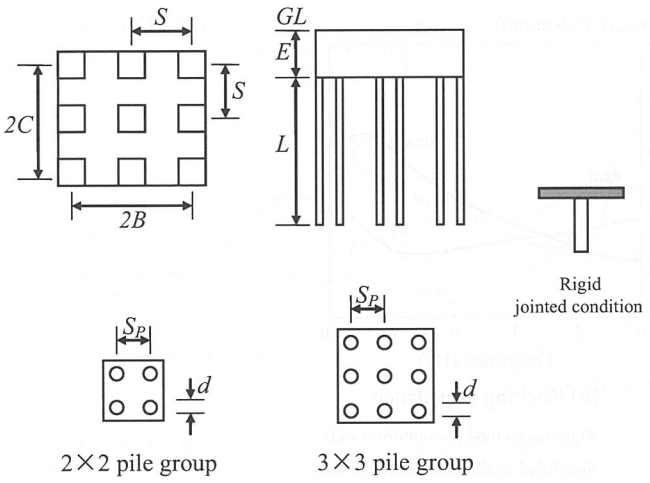

Fig. 13. Layout of the embedded foundation supported by pile groups.

moment cannot be transmitted through the pin-jointed point) between the pile head and the foundation under non-uniform soil conditions. The layouts of the raft and embedded foundations supported by pile groups are shown in Fig. 16.

The parameters of the raft and embedded foundations are similar to those depicted in Section 3.1. However, the pin-jointed condition between the pile head and the foundation is used, as depicted in Fig. 16.

Fig. 17 shows the dynamic impedance and foundation input motion for raft foundations with 2 × 2 and 3 × 3 pile groups using the simplified and rigorous methods. The results show notably good agreement for the 2 × 2 and 3 × 3 pile groups with a pin-jointed condition between the pile head and the foundation. A minor difference was generated in the high-frequency domain.

Fig. 18 shows the dynamic impedance and foundation input motion of embedded foundations with 2 × 2 and 3 × 3 pile groups. The results obtained from the simplified and rigorous methods are nearly identical for the embedded foundations supported by pile groups with pin-jointed conditions between the pile head and the foundation.

3.3. Simplified method employed in a large piles group

The applicability of the proposed simplified method for a large pile group is presented in Fig. 19(a). Three cases, as depicted in Fig. 19, are investigated in this section. In Case 1, a large pile group is meshed by 4 × 4 blocks (uniformly spaced mesh). In Case 2, a large pile group is meshed by 4 × 4 blocks (irregularly spaced mesh). In Case 3, a large pile group is meshed by 2 × 2 blocks (uniformly spaced mesh). The piles in each block are aggregated into one equivalent pile. The diameter of the pile is 1.2 m and has a length of 20 m. The piles are placed at a spacing of 2.5*d* (*S*). The impedances and foundation input motions are evaluated through the simplified method and compared with those obtained from the rigorous method, as shown in Fig. 20. Fig. 20 shows that the results are in very good agreement for Cases 1 and 2 from 0 to 6 Hz. In the high-frequency domain (>6 Hz), a minor difference is

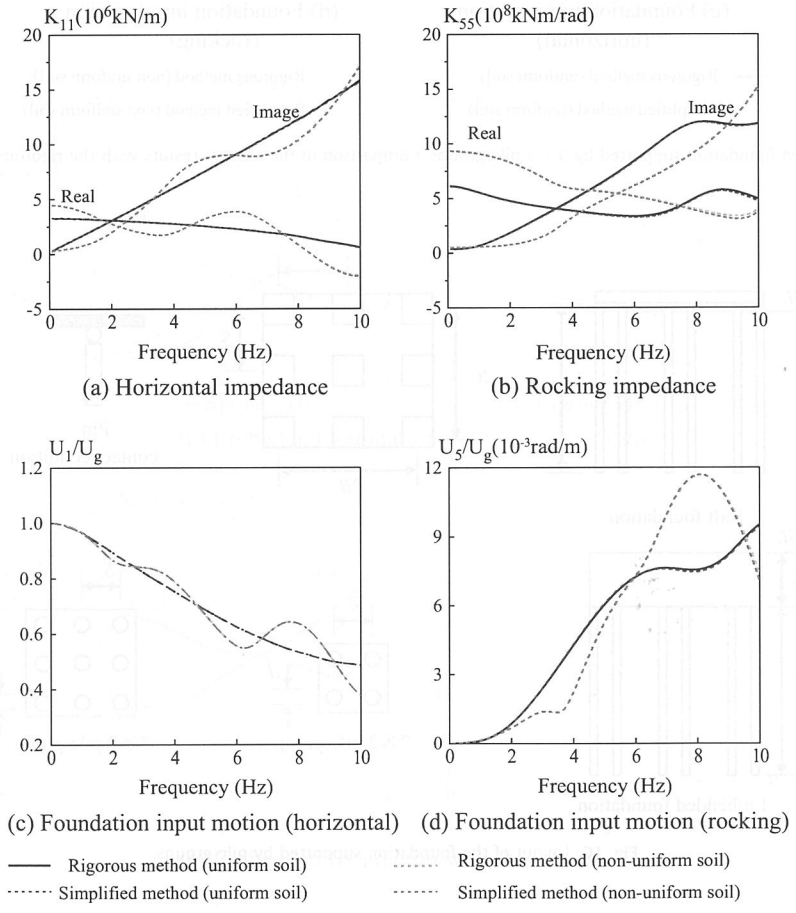

Fig. 14. Embedded foundation supported by 2 × 2 pile groups. Comparison of the current results with the rigorous method solution.

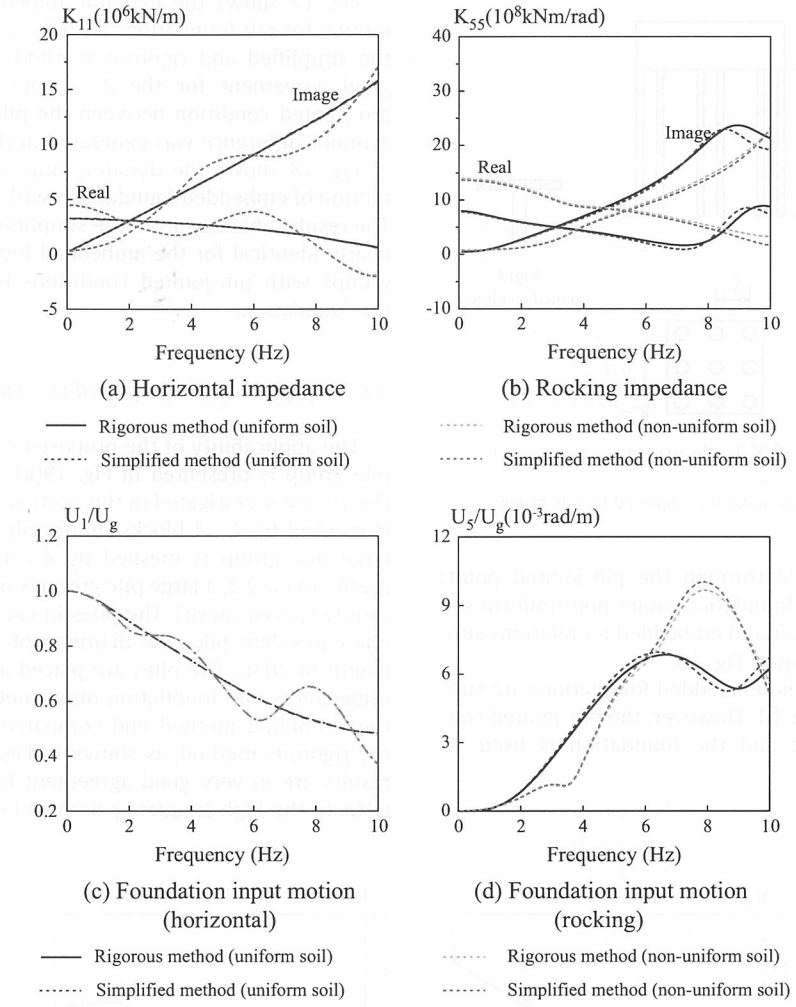

Fig. 15. Embedded foundation supported by 3 × 3 pile groups. Comparison of the current results with the rigorous method solution.

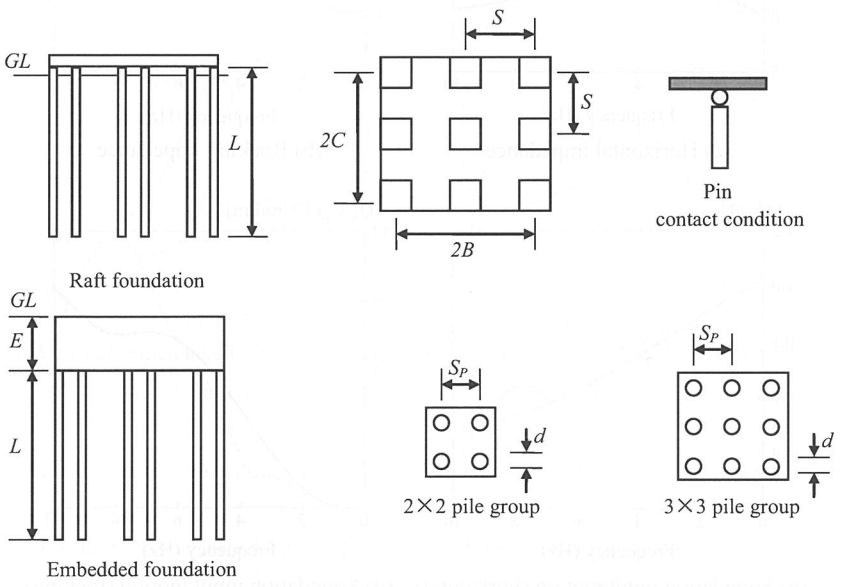

Fig. 16. Layout of the foundation supported by pile groups.

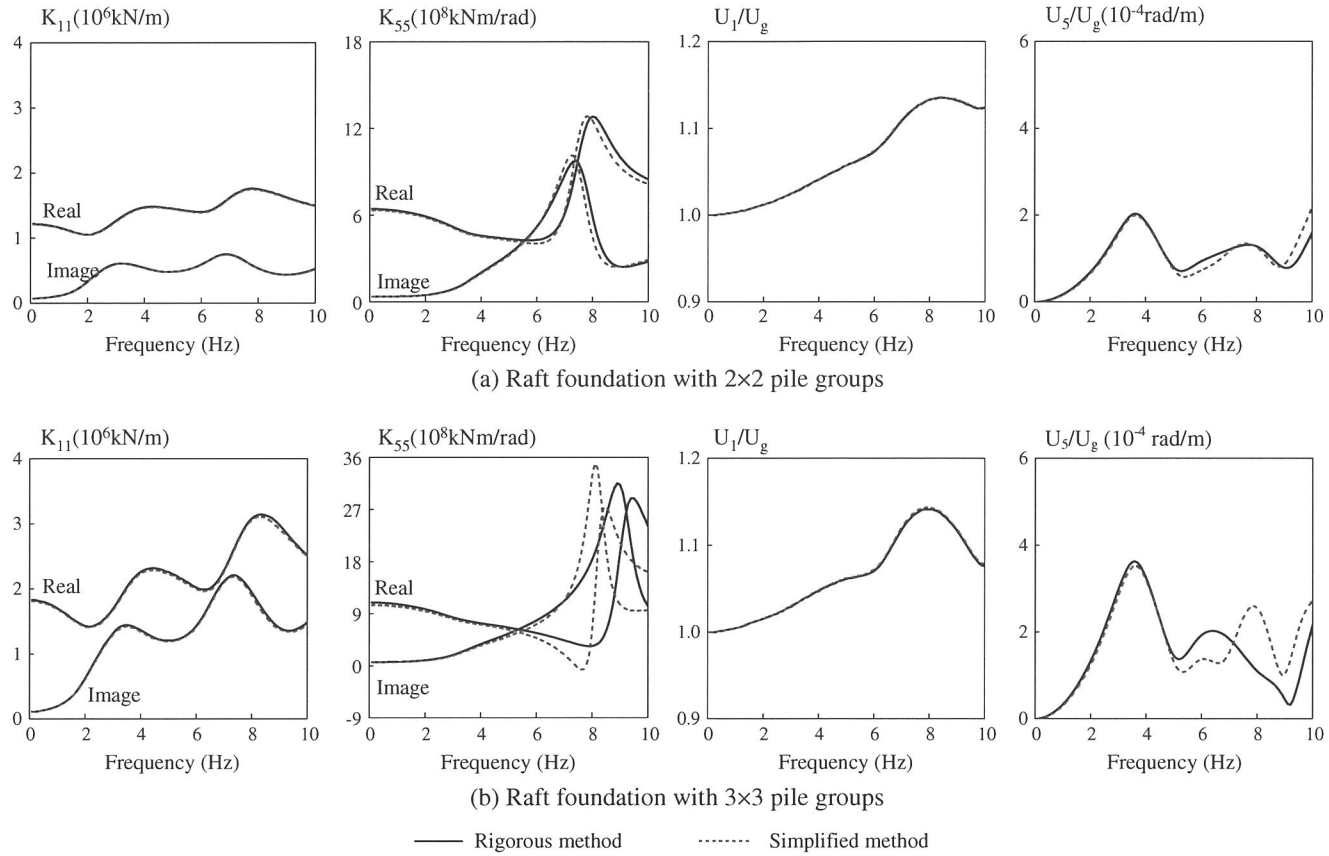

Fig. 17. Raft foundation supported by 2 × 2 and 3 × 3 pile groups. Comparison of the current results with the rigorous method solution.

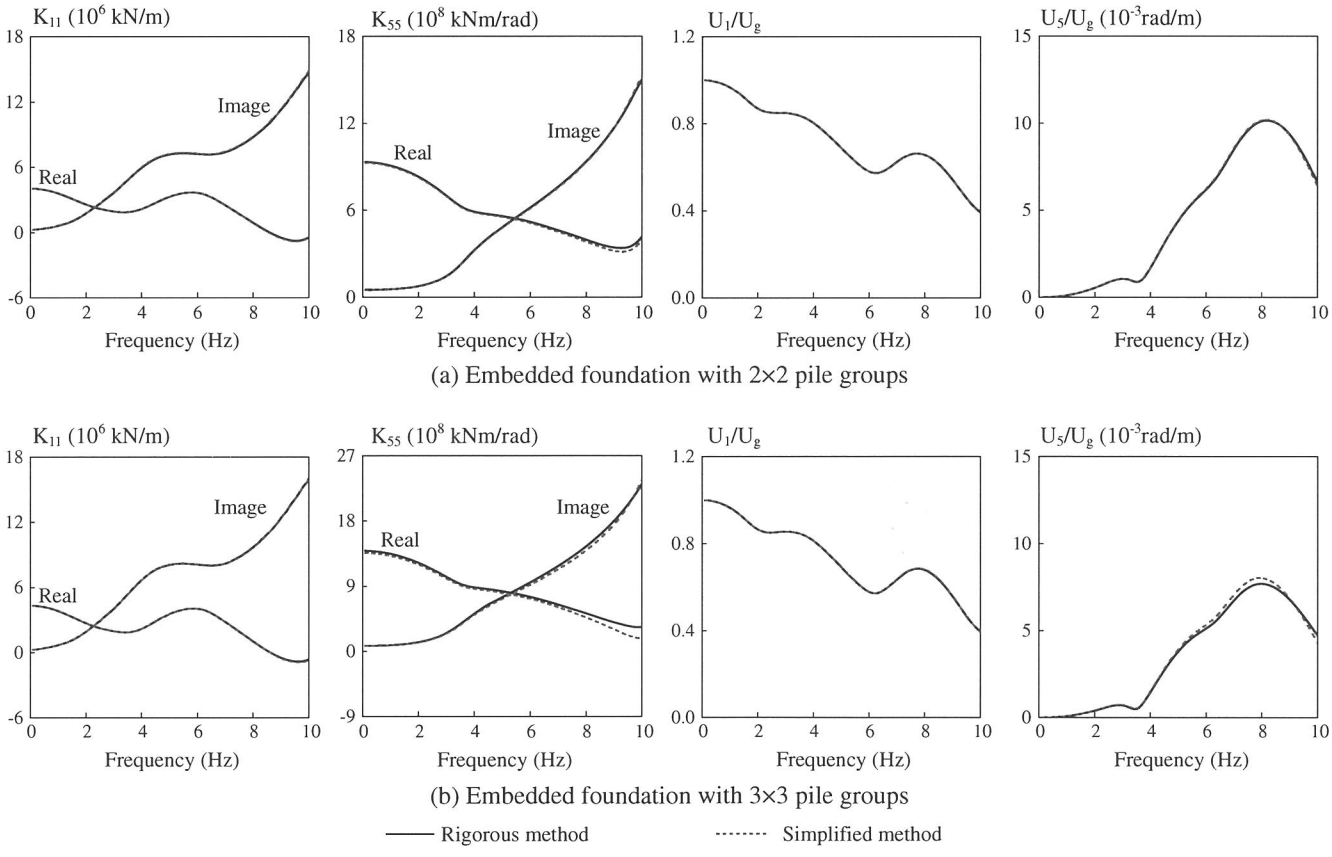

Fig. 18. Embedded foundation supported by 2 × 2 and 3 × 3 pile groups. Comparison of the current results with the rigorous method solution.

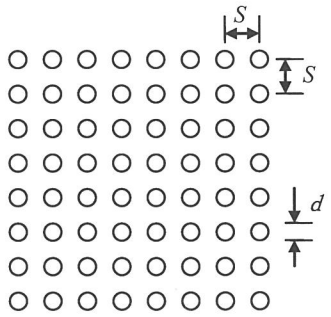

(a) Large pile groups

Pile parameters	
d=1.2m	E_P=2.1×10^{7}kN/m^2
s=2.5d	ρ_P=2.4t/m^3
L=20m	h_P=0.03

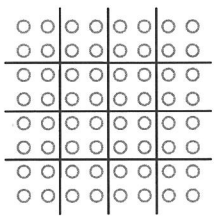

(b) Case 1: 4 x 4 block (Uniformly spaced mesh)

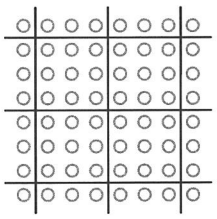

(c) Case2: 4 x 4 block (Irregularly spaced mesh)

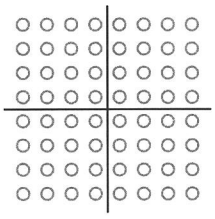

(d) Case3: 2 x 2 block (Uniformly spaced mesh)

Fig. 19. Layout of large pile group.

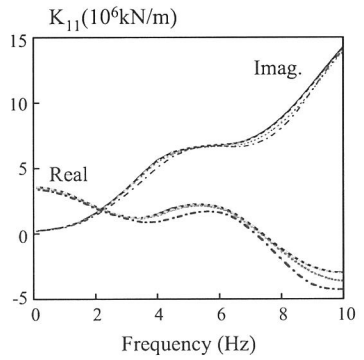

(a) Horizontal impedance

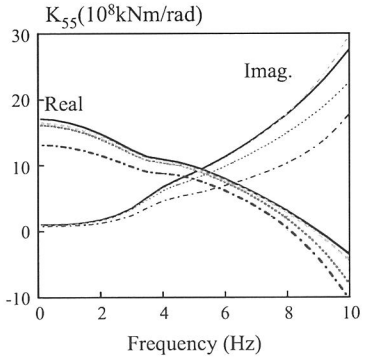

(b) Rocking impedance

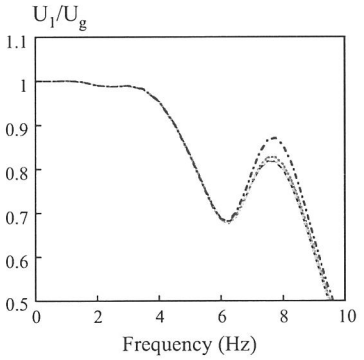

(c) Foundation input motion (horizontal)

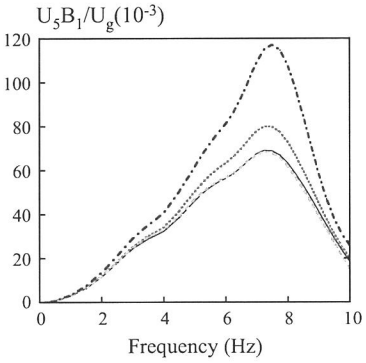

(d) Foundation input motion (rocking)

Solution of rigorous method
Case 2: Solution of simplified method
Case 1: Solution of simplified method
Case 3: Solution of simplified method

Fig. 20. Impedances and foundation input motions of large pile group. Comparison of present results with those of rigorous method.

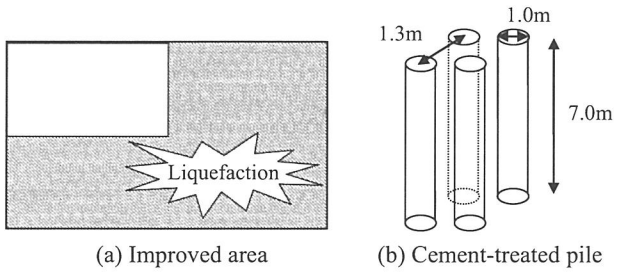

Fig. 21. Sketch of the ground improvement.

generated between the solutions of the simplified and rigorous methods, particularly for the rocking impedance and foundation input motion (rocking). For Case 3, the large pile group is meshed into four blocks. The piles in each block are aggregated into one equivalent pile. The calculation efficiency of the simplified method decreases in this case, particularly for the rocking direction, because the ratio of the area of each block to the area of the large pile group is large. For Case 3, the difference is approximately 23% for the rocking impedance, whereas for Case 1, the difference is approximately 4%. Theoretically, as we know, the rocking stiffness is proportional to the moment of the inertial area. Thus, if the large

Table 1
Parameters of the soil and cement–soil pile.

	Depth GL (m)	Vs m/s	Density g/cm^3	Poisson's ratio
0.00 m				
Soil	0.00 – 1.50	160	1.80	0.410
	1.50 – 1.95	160	1.70	0.410
	1.95 – 5.30	250	2.00	0.357
	5.30 – 10.00	210	1.80	0.456
	10.00 – 13.95	310	2.00	0.459
	13.95 – 16.95	270	1.90	0.486
	16.95 – 20.30	220	1.90	0.491
	20.30 – 25.25	270	2.00	0.486
	25.25 – 32.70	300	2.10	0.483
	32.70 – 38.70	280	1.80	0.484
	38.70 – 44.55	280	1.70	0.484
	44.55 – 49.35	420	2.10	0.474
	49.35 – 58.50	710	2.10	0.448
	58.50 – 62.00	500	2.10	0.468
	62.00 – 67.00	540	2.10	0.463
	67.00 – 68.75	330	1.70	0.479
	68.75 – 71.50	330	1.90	0.479
71.50 m	71.50 – 75.00	300	1.80	0.483
Cement–Soil Pile		820	2.00	0.300

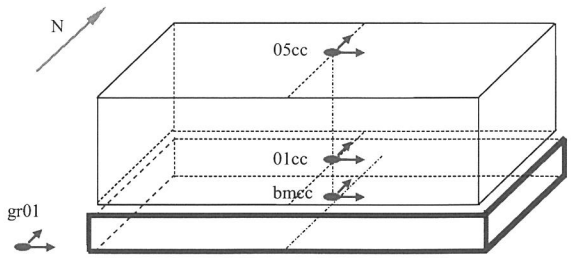

Parameters of the accelerometer
Accelerometers type:
Force balance servo accelerometer
Dynamic range: 155dB
Frequency range: DC~200Hz
Trigger threshold value: 0.5gal

Fig. 22. Accelerometer sensor locations.

pile group is divided into n blocks, the difference in the rocking stiffness calculated using the simplified method is $1/n^2$. Through a comparison of the results, as depicted in Fig. 19(b), our conclusion is validated.

Therefore, to increase the accuracy of the simplified method, the area of the meshed block should be sufficiently smaller than that of the large pile group. Thus, considering the balance between the computation time and the calculation accuracy, the pile group should be divided into $4 \times 4 \sim 6 \times 6$ blocks.

The effectiveness of the simplified method has been validated in this section. In the succeeding section, the dynamic response of an actual structure is investigated with consideration of the soil–structure interaction. An embedded foundation resting on 2203 cement–soil piles was employed as the structure. The proposed simplified method was used to model the 2203 cement–soil piles for analysis of the dynamic response of the structure with consideration of the soil–structure interaction.

4. Use of the simplified method in analysis of the dynamic response of an actual structure

4.1. Description of the structure

The subject structure is a base-isolated, four-story, reinforced-concrete frame structure. The superstructure is supported with rubber base isolators that rest on the foot foundations. The superstructure has side lengths of 100 m and 50 m in the x and y directions, respectively. The heights of the stories are as follows: basement, 3 m; first floor, 5.5 m; second and third floors, 4.8 m; and fourth floor, 4.5 m. The weights of each floor from the basement to the roof of the structure are 2.09×10^4 tons, 9.58×10^3 tons, 6.39×10^3 tons, 6.66×10^3 tons, 7.02×10^3 tons, and 5.96×10^3 tons. The stiffnesses of the structure in (x, y) are as follows: isolation system (0.42×10^{10} N/m, 0.42×10^{10} N/m); first floor (1.79×10^{10} N/m, 1.78×10^{10} N/m); second floor (1.79×10^{10} N/m, 1.74×10^{10} N/m); third floor (1.84×10^{10} N/m, 1.92×10^{10} N/m); and fourth floor (1.81×10^{10} N/m, 1.78×10^{10} N/m).

4.2. Soil-foundation system

An embedded foundation with an embedded depth of 4.0 m was used, with planar dimensions of approximately 52 m × 104 m. The results of a soil investigation conducted prior to structure construction showed that 75% of the soil area under the foundation (shadowed area in Fig. 21) might liquefy if exposed to strong ground motions. Soil liquefaction, which results from a build-up of excess pore water pressure in loose saturated soils, leads to a critical loss of soil strength and stiffness and consequently to unacceptably large deformations. To reduce the potential hazards posed by soil liquefaction, the cement-treated ground improvement technique was applied in the shadowed area. The ground improvement area consists of 2203 cement–soil piles 7 m long and 1.0 m in diameter, with a 1.3-m center-to-center pile spacing. A parallel-seismic (PS) test and boring investigation were conducted in the improved and unimproved areas, and the results are shown in Table 1.

4.3. Observation system

Immediately after construction, the structure and free field were permanently implanted with strong motion accelerometers. Two unidirectional horizontal accelerometers were installed orthogonally in the center of the roof, the first floor, and the basement to capture the transverse and longitudinal responses of the

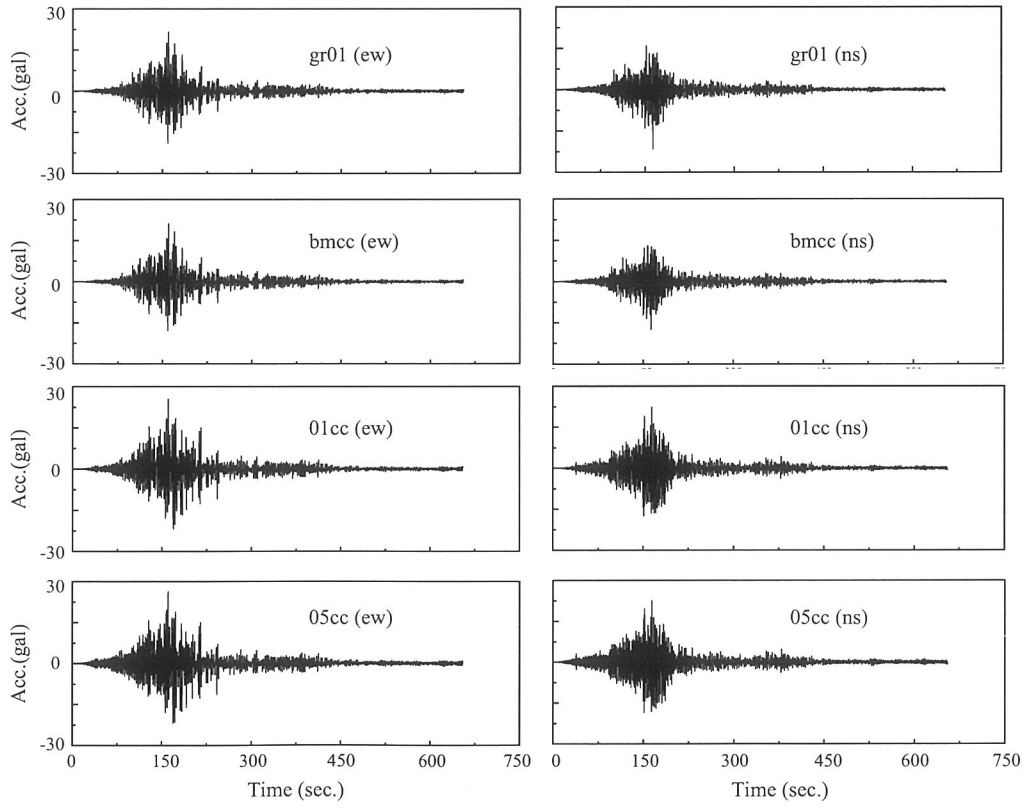

Fig. 23. Selected acceleration records.

Table 2
Amplitude of the selected acceleration records (Abs(gal)).

Direction	gr01	bmcc	01 cc	05 cc
ew	21.68	21.14	25.45	26.32
ns	21.62	17.46	22.34	22.59

structure. Two unidirectional horizontal accelerometers were installed in the free field adjacent to the building to observe the seismic response of the ground induced by an earthquake. Detailed information on the accelerometers, including their locations, is provided in Fig. 22. The symbols *gr*, *bm*, 01, and 05 indicate the free field, basement, first floor, and roof, respectively. The symbol *cc* denotes the location at the center of each floor. The horizontal response of the structure was obtained from the accelerometers located at the center of each floor. Using the observation system sketched in Fig. 22, the responses of the structure in the horizontal direction can be obtained simultaneously during earthquake excitation.

4.4. Selected acceleration records

The observation system previously recorded the motions (Fig. 23) of a magnitude 9.0 earthquake that occurred in Pacific coast of Tohoku, Japan, on March 11, 2011. This earthquake

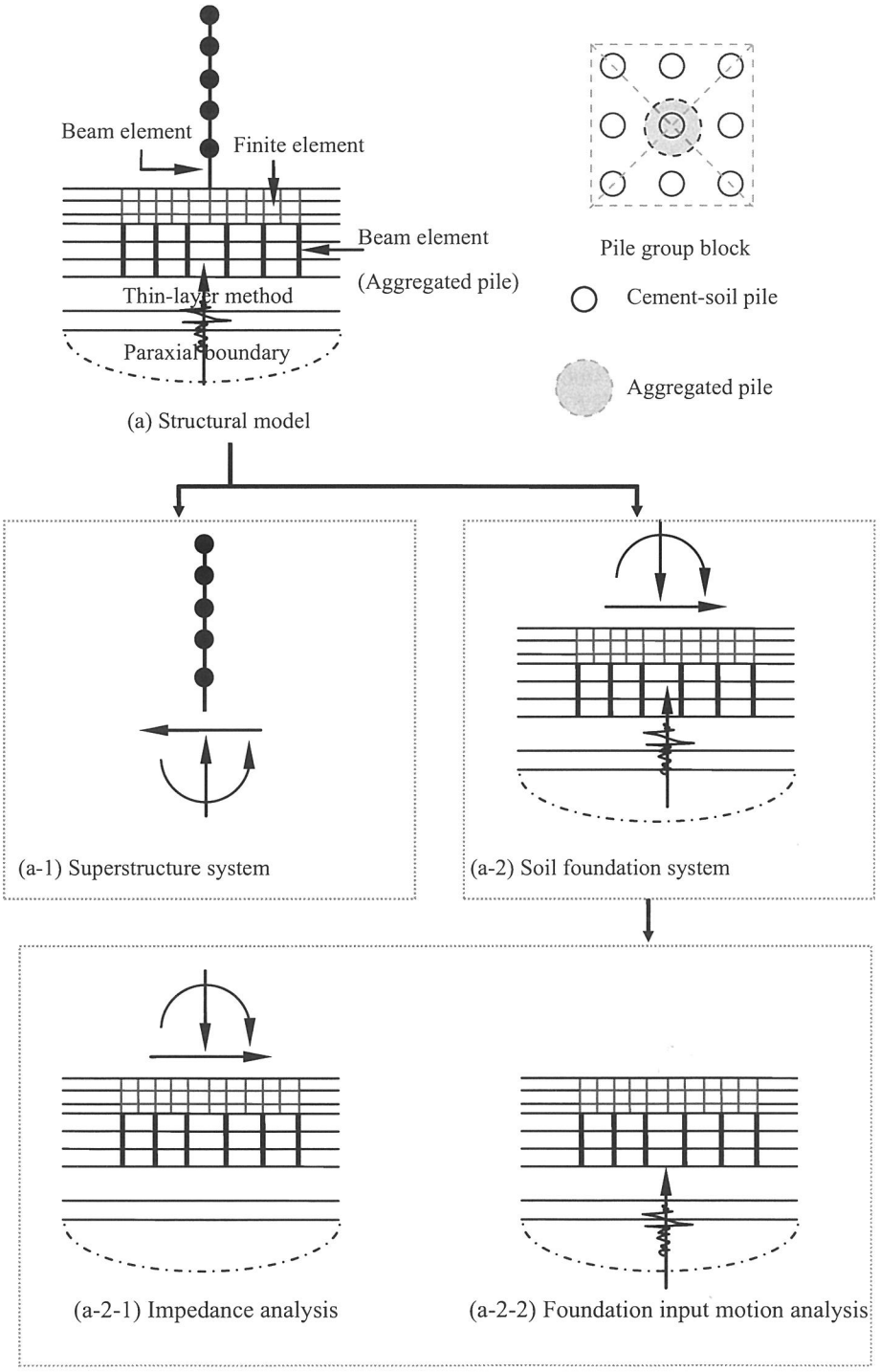

Fig. 24. Structural model considering soil structure interaction.

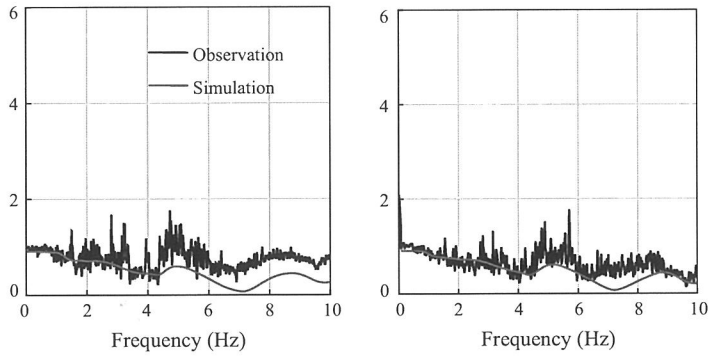

(a) U_{BF}/U_g(NS) (b) U_{BF}/U_g(EW)

Note: BF is the foundation of the building, and g is the free field of the foundation

Fig. 25. Transfer function of the soil-foundation system.

induced ground accelerations of less than 22 *gals*. The recorded data were used to analyze the dynamic characteristic of the base-isolated structure in this study. The characteristics of the records shown in Fig. 23 are summarized in Table 2.

4.5. Considered structural model

The well-known beam model is one of the most commonly used models for conducting comprehensive parametric studies. In the MDOF structure models used in this study, each floor is assumed to be a lumped mass connected by a beam element. The weight of the lumped mass and the stiffness of the beam element were given previously in Section 4.1. The 2203 cement–soil piles should be modeled to consider the soil–structure interaction. However, due to the massive number of cement–soil piles, the simplified method was used to model the cement–soil piles, and nine cement–soil pile groups were aggregated to one to reduce the number of degrees of freedom. The pin-jointed condition was applied between the pile head and the foundation.

This idealized model is shown in Fig. 24. As shown in Fig. 24(a), using the substructure method, the structure model can be divided into a superstructure system and a soil foundation system. Using

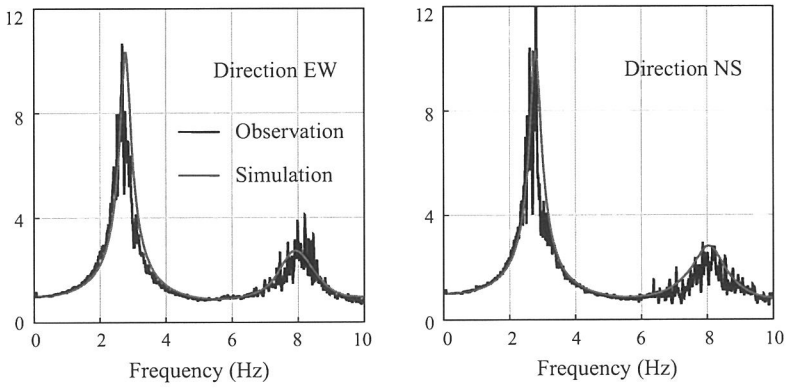

(a) Transfer function: U_{RF}/U_{1F}

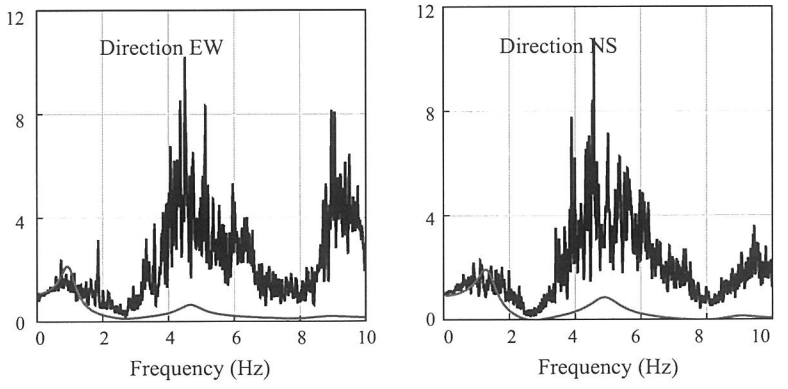

(b) Transfer function: U_{1F}/U_{BF}

Note: RF-the roof of the building, 1F-the first floor of the building, BF-the basement of the building

Fig. 26. Transfer function of the superstructure.

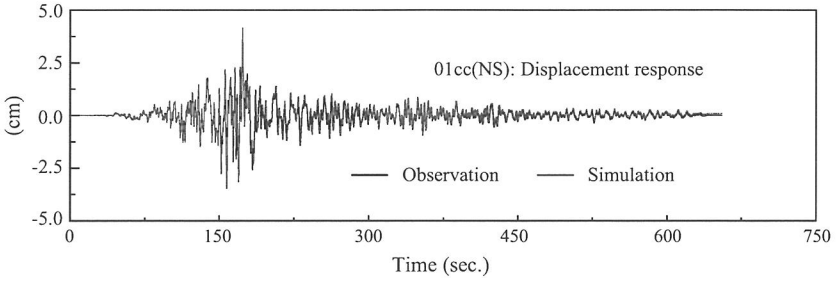

Fig. 27. Absolute displacement response of the subject structure in the time domain (including the displacement of the free field ($x_g(t)$)).

the superposition principle, the soil foundation system can again be decomposed into the impedance analysis and foundation input motion analysis problem, which can be calculated using the proposed simplified method described in Section 2.2. Using the obtained impedance and foundation input motion as the boundary condition and excitation source of the superstructure, the dynamic response of the superstructure can be analyzed.

4.6. Comparison of the numerical analysis results and observation data

Transfer functions can be visualized to represent the characteristics of a system that receives input x modified to output y. In the kinematic soil–structure interaction, input x is the free-field motion, and output y is the base-mat motion. In the superstructure, input x is the first floor and y is the roof. The auto- and cross-power spectral functions of the input and output signals were used to estimate the complex-valued transfer function indicated below.

$$H_v(\omega) = \frac{S_{xy}(\omega)}{|S_{xy}(\omega)|} \times \sqrt{\frac{S_{yy}(\omega)}{S_{xx}(\omega)}} \tag{16}$$

where $S_{xx}(w)$ and $S_{yy}(w)$ represent the auto-power spectral functions of the input and output signals, respectively, and $S_{xy}(w)$ is the cross-power spectral function. The actual dynamic characteristics of the building during the Naraken earthquake were estimated based on the simulated (using the structural model discussed in Section 4.5) and recorded transfer functions. The recorded and simulated transfer functions obtained from the basement/free field in the NS and EW directions are shown in Fig. 25, and the agreement between the simulated and recorded results is satisfactory. Hence, the proposed simplified method is effective for establishing the soil-foundation model and analyzing the effect of the soil–structure interaction.

Fig. 26 shows the recorded and simulated roof/first floor and first floor/basement transfer functions. A comparison of the simulated and identified periods indicates good agreement. The amplitude of the simulated and recorded transfer functions approximately represents the first-mode frequency. However, certain differences exist between the transfer function($U_{1\,F}/U_{BF}$) ordinates at the second-mode frequency, the observed difference in the transfer functions for the simulated and observed results should be investigated in future work.

Fig. 27 shows a comparison of the results of the recorded and simulated displacements for the first floor in the NS direction, and good agreement was achieved.

5. Conclusion

A simplified method was developed to estimate the dynamic impedance and foundation input motion of a foundation with a large number of piles. To verify the efficiency of the simplified method, the results of the impedance and foundation input motion obtained from the simplified and rigorous method solutions were investigated and compared. The main conclusions drawn from the investigation are as follows:

(1) The impedance and foundation input motion can be estimated using the simplified method, and thus, the memory requirements for the computation and the calculation time can be minimized. For example, a group of m piles is aggregated into one equivalent pile. The number of degrees of freedom of the piles in the group is reduced to $1/m$, and the computer memory requirement is reduced to $1/m^2$. Therefore, analysis of the dynamic characteristics of a foundation with a large number of piles is easier with the simplified method.
(2) The simplified and rigorous method solutions are nearly identical for the impedance and foundation input motion in the horizontal direction. A difference generated in the high-frequency domain for the impedance and foundation input motion in the rocking direction tends to increase for an increasing number of piles in the group. However, in the low-frequency range, the simplified and rigorous methods are similar to each other.
(3) The foundation input motion was predicted via the simplified method for an actual structure. The results indicate that the proposed simplified method is useful for the seismic design of structures with a large number of piles with consideration of the soil–structure interaction.

Acknowledgements

The authors gratefully acknowledge financial support provided by the National Natural Science Foundation of China (Grant No. 51308243) and the National Basic Research Program (973) of China (Grant No. 2011CB013800).

Appendix A. Formulation of the Green's function used in the thin layer method and expression of the paraxial boundary condition

The displacement solution of a point located at R surface for the load acting at S surface (see Fig. A.1) includes:

(1) Point load solution($r > 0$);
(2) Disk load solution($r \to 0$, pile tip);
(3) Ring load solution($r \to 0$, pile shaft);

A.1. Point load solution

Let $u_x, u_y u_z$ = displace components at elevation R for a point load acting at elevation S. The Green's function for point load is:

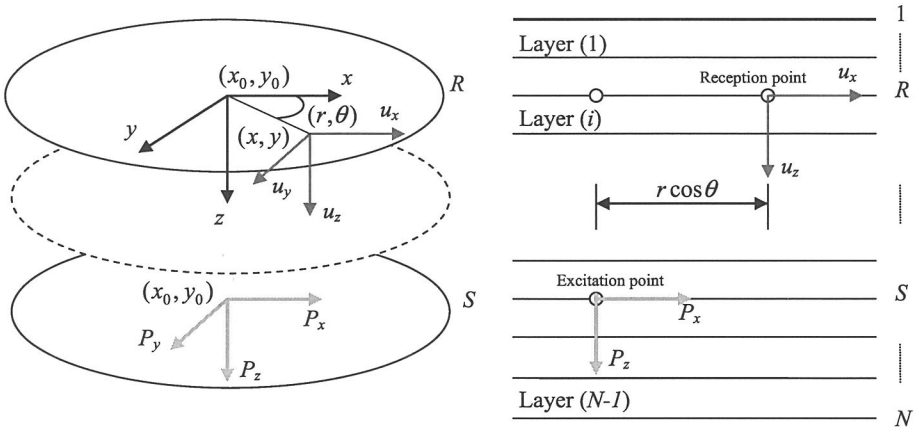

Fig. A.1. Geometric relationship between the excitation point and reception point in the thin layered method.

$$\begin{Bmatrix} u_x \\ u_y \\ u_z \end{Bmatrix}_R = \begin{bmatrix} V_1\cos 2\theta + V_2 & V_1 \sin 2\theta & V_4 \cos\theta \\ V_1 \sin 2\theta & -V_1 \cos 2\theta + V_2 & V_4 \sin\theta \\ -V_3 \cos\theta & -V_3 \sin\theta & V_5 \end{bmatrix} \begin{Bmatrix} P_x \\ P_y \\ P_z \end{Bmatrix}_S \tag{A.1}$$

where:

$$V_1 = -\frac{1}{2\pi}\sum_{k=1}^{2N}\frac{X_{Rk}X_{Sk}}{D_{k\alpha}}\alpha_k^2 F_1(\alpha_k r) + \frac{1}{4\pi}\sum_{k=1}^{N}\frac{Y_{Rk}Y_{Sk}}{D_{k\beta}}F_1(\beta_k r)$$

$$V_2 = \frac{1}{2\pi}\sum_{k=1}^{2N}\frac{X_{Rk}X_{Sk}}{D_{k\alpha}}\alpha_k^2 F_2(\alpha_k r) + \frac{1}{4\pi}\sum_{k=1}^{N}\frac{Y_{Rk}Y_{Sk}}{D_{k\beta}}F_2(\beta_k r)$$

$$V_3 = \frac{1}{\pi}\sum_{k=1}^{2N}\frac{Z_{Rk}X_{Sk}}{D_{k\alpha}}\alpha_k^2 F_3(\alpha_k r)$$

$$V_4 = \frac{1}{\pi}\sum_{k=1}^{2N}\frac{X_{Rk}Z_{Sk}}{D_{k\alpha}}\alpha_k^2 F_3(\alpha_k r)$$

$$V_5 = \frac{1}{\pi}\sum_{k=1}^{2N}\frac{Z_{Rk}Z_{Sk}}{D_{k\alpha}}\alpha_k^2 F_2(\alpha_k r)$$

$$F_1(z) = -\frac{2}{z^2} - i\frac{\pi}{z}H_1^{(2)}(z) + i\frac{\pi}{2}H_0^{(2)}(z)$$

$$F_2(z) = -i\frac{\pi}{2}H_0^{(2)}(z)$$

$$F_3(z) = -i\frac{\pi}{2}H_0^{(2)}(z)$$

$$D_{k\alpha} = -\{X\}_k^T[E_S]\{X\}_k - \{Z\}_k^T[E_P]\{Z\}_k + \alpha_k^2\{X\}_k^T[A_P]\{X\}_k + \alpha_k^2\{Z\}_k^T[A_S]\{Z\}_k$$

$$D_{k\beta} = \{Y\}_k^T[A_S]\{Y\}_k$$

$$r = \sqrt{(x-x_0)^2 + (y-y_0)^2}$$

$$\theta = a\tan\left(\frac{y-y_0}{x-x_0}\right)$$

$H_\nu^{(2)}(z)$ is the second Hankel function of order ν.
α_k is the kth eigenvalue of characteristic equation (A.4).
β_k is the kth eigenvalue of characteristic equation (A.5).
X_k, Z_k is the corresponding eigenvector of α_k.
Y_k is the corresponding eigenvector of β_k.
X_{Rk} is the Rth component of the eigenvector X_k.
Z_{Rk} is the Rth component of the eigenvector Z_k.
Y_{Rk} is Rth component of the eigenvector Y_k.

A.2. Disk load solution

Let $u_x, u_y u_z$ = displace components at elevation R for a disk load acting at elevation S. The Green's function for disk load is then

$$\begin{Bmatrix} u_x \\ u_y \\ u_z \end{Bmatrix}_R = \begin{bmatrix} V_6(r=r_0) & & \\ & V_6(r=r_0) & \\ & & V_7(r=r_0) \end{bmatrix} \begin{Bmatrix} P_x \\ P_y \\ P_z \end{Bmatrix}_S \tag{A.2}$$

where

$$V_6 = \frac{1}{2\pi}\sum_{k=1}^{2N}\frac{X_{Rk}X_{Sk}}{D_{k\alpha}}\alpha_k^2 F_4(\alpha_k r) + \frac{1}{4\pi}\sum_{k=1}^{N}\frac{Y_{Rk}Y_{Sk}}{D_{k\beta}}F_4(\beta_k r)$$

$$V_7 = \frac{1}{\pi}\sum_{k=1}^{2N}\frac{Z_{Rk}Z_{Sk}}{D_{k\alpha}}\alpha_k^2 F_4(\alpha_k r)$$

$$F_4(z) = -\frac{2}{z^2} - i\frac{\pi}{2}H_1^{(2)}(z)$$

r_0 is the radius of the disk

A.3. Ring load solution

$$\begin{Bmatrix} u_x \\ u_y \\ u_z \end{Bmatrix}_R = \begin{bmatrix} V_2(r=r_0) & & \\ & V_2(r=r_0) & \\ & & V_5(r=r_0) \end{bmatrix} \begin{Bmatrix} P_x \\ P_y \\ P_z \end{Bmatrix}_S \tag{A.3}$$

where

$$V_2 = \frac{1}{2\pi}\sum_{k=1}^{2N}\frac{X_{Rk}X_{Sk}}{D_{k\alpha}}\alpha_k^2 F_2(\alpha_k r) + \frac{1}{4\pi}\sum_{k=1}^{N}\frac{Y_{Rk}Y_{Sk}}{D_{k\beta}}F_2(\beta_k r)$$

$$V_5 = \frac{1}{\pi}\sum_{k=1}^{2N}\frac{Z_{Rk}Z_{Sk}}{D_{k\alpha}}\alpha_k^2 F_2(\alpha_k r)$$

$$F_2(z) = -i\frac{\pi}{2}H_0^{(2)}(z)$$

r_0 is the radius of the ring

A.4. Characteristic equation of the thin layer model as shown in Fig. A.1

The characteristic equations of the thin layer model (shown in Fig. 1) for Rayleigh (in-plane) and Love (anti-plane) waves are expressed by equations (A.4) and (A.5), respectively.

$$\left(\alpha^2\begin{bmatrix}[A_P] & \\ & [A_S]\end{bmatrix} + \alpha\begin{bmatrix}[B] & \\ [B]^T & \end{bmatrix} + \begin{bmatrix}[E_S] & \\ & [E_P]\end{bmatrix}\right)\begin{Bmatrix} X \\ Z \end{Bmatrix} = \{0\} \tag{A.4}$$

$$\left(\beta^2[A_S] + [E_S]\right)\{Y\} = \{0\} \tag{A.5}$$

where $[A_S], [A_P]$, $[E_S], [E_P]$, and $[B]$ are the matrices assembled by $[A_S]^{(i)}, [A_P]^{(i)}, [E_S]^{(i)}, [E_P]^{(i)}$ and $[B]^{(i)}$, respectively, in the manner presented in equation (A.6).

$$[A]=\begin{bmatrix} A_{11}^{(1)} & A_{12}^{(1)} & & & & & \\ A_{21}^{(1)} & A_{22}^{(1)}+A_{11}^{(2)} & A_{21}^{(2)} & & & & \\ & A_{12}^{(2)} & A_{22}^{(2)}+A_{11}^{(3)} & & & & \\ & & & \ddots & & & \\ & & & a_{22}^{(N-3)}+A_{11}^{(N-2)} & A_{12}^{(N-2)} & & \\ & & & A_{21}^{(N-2)} & A_{22}^{(N-2)}+A_{11}^{(N-1)} & A_{12}^{(N-1)} & \\ & & & & A_{21}^{(N-1)} & A_{22}^{(N-1)}+A^{(N)} \end{bmatrix} \tag{A.6}$$

where $A^{(i)}$ is the matrix corresponding to the i-th soil layer, and $A^{(N)}$ is matrix corresponding to the boundary condition.

$$[A_S]^{(i)}=\frac{G_iH_i}{6}\begin{bmatrix}2&1\\1&2\end{bmatrix}$$

$$[A_P]^{(i)}=\frac{(\lambda_i+2G_i)H_i}{6}\begin{bmatrix}2&1\\1&2\end{bmatrix}$$

$$[E_S]^{(i)}=[G_S]^{(i)}-\omega^2[M]^{(i)}$$

$$[G_S]^{(i)}=\frac{G_i}{H_i}\begin{bmatrix}1&-1\\-1&1\end{bmatrix}$$

$$[M]^{(i)}=\frac{\rho_iH_i}{6}\begin{bmatrix}2&1\\1&2\end{bmatrix}$$

$$[E_P]^{(i)}=[G_P]^{(i)}-\omega^2[M]^{(i)}$$

$$[G_P]^{(i)}=\frac{(\lambda_i+2G_i)}{H_i}\begin{bmatrix}1&-1\\-1&1\end{bmatrix}$$

$$[B]^{(i)}=\begin{bmatrix}-(\lambda_i-G_i)/2 & (\lambda_i+G_i)/2\\ -(\lambda_i+G_i)/2 & (\lambda_i-G_i)/2\end{bmatrix}$$

where ω is the excited frequency of the load, and $\lambda_i, G_i, H_i, \rho_i$ are the Lame constant, shear elastic modulus, thickness and density of the ith soil layer, respectively.

α_k and $\{X_k \;\; Z_k\}^T(k=1,2\ldots2N)$ represent the eigenvalue and eigenvector, respectively, of characteristic equation (A.4).

β_k and $\{Y_k\}^T(k=1,2\ldots N)$ represent the eigenvalue and eigenvector, respectively, of the characteristic equation (A.5).

A.5. Paraxial boundary

① The boundary condition of equation (A.5) is as follows:

$$A_S^N=-i\frac{G_N}{2}\frac{V_{SN}}{\omega} \tag{A.7}$$

$$E_S^N=i\omega\rho_NV_{SN} \tag{A.8}$$

② The boundary condition of equation (A.4) is shown as follows:

$$A_S^N=i\frac{G_N}{2}\frac{V_{SN}}{\omega}\eta_N^2(\eta_N-2)=i\frac{\lambda_N+2G_N}{2}\frac{V_{SN}}{\omega}(\eta_N-2) \tag{A.9}$$

$$A_P^N=i\frac{G_N}{2}\frac{V_{SN}}{\omega}(1-2\eta_N) \tag{A.10}$$

$$B^N=G_N(2-\eta_N) \tag{A.11}$$

$$E_S^N=i\omega\rho_NV_{SN} \tag{A.12}$$

$$E_P^N=i\omega\rho_NV_{PN} \tag{A.13}$$

where

$$\eta_N=\frac{V_{PN}}{V_{SN}}$$

$$\lambda_N=\frac{2\nu_N}{1-2\nu_N}G_N$$

$$G_N=\rho_NV_{SN}^2$$

$\lambda_N, G_N, \rho_N, \nu_N, V_{SN}$, and V_{PN} are the Lame constant, shear elastic modulus, density, Poisson ratio, S-wave velocity and P-wave velocity of the boundary, respectively.'

References

[1] Kaynia AM. Dynamic stiffness and seismic response of pile groups. Massachusetts: Massachusetts Institute of Technology; 1982. Report No.: R83-03.

[2] Kaynia AM, Kausel E. Dynamics of piles and pile groups in layered soil media. Soil Dyn Earthq Eng 1991;10(8):386–401.

[3] Gazetas G, Fan K, Kaynia AM, Kausel E. Dynamic interaction factors for floating pile groups. J Geotech Eng ASCE 1991;117(10):1531–48.

[4] Kaynia AM, Novak M. Response of pile foundations to Rayleigh waves and obliquely incident body waves. Earthq Eng Struct Dyn 1992;21(4):303–18.

[5] Miura K, Kaynia AM, Masuda K, Kitamura E, Seto Y. Dynamic behaviour of pile foundations in homogeneous and non-homogeneous media. Earthq Eng Struct Dyn 1994;23(2):183–92.

[6] Davies TG, Sen R, Banerjee PK. Dynamic behavior of pile groups in inhomogeneous soil. J Geotech Eng 1985;111(12):1365–79.

[7] Mamoon SM, Kaynia AM, Banerjee PK. Frequency domain dynamic analysis of piles and pile groups. J Eng Mech ASCE 1990;116(10):2237–57.

[8] Ottaviani M. Three dimensional finite element analysis of vertically loaded pile groups. Geotechnique 1975;25(2):159–74.

[9] Sheng DC, Eigenbrod KD, Wriggers P. Finite element analysis of pile installation using large-slip frictional contact. Comput Geotech 2005;32(1):17–26.

[10] Poulos HG, Davis EH. Pile foundation analysis and design. New York: Wiley; 1980.

[11] Butterfield R, Banerjee PK. The elastic analysis of compressible piles and pile groups. Geotechnique 1971;21(1):43–60.

[12] Mandolini A, Viggiani C. Settlement of piled foundations. Geotechnique 1997;47(4):791–816.

[13] Xu KJ, Poulos HG. General elastic analysis of piles and pile groups. Int J Numer Anal Methods Geomech 2000;24(15):1109–38.

[14] Almeida VS, de Paiva JB. Static analysis of soil/pile interaction in layered soil by BEM/BEM coupling. Adv Eng Softw 2007;38(11–12):835–45.

[15] Dobry R, Gazetas G. Simple method for dynamic stiffness and damping of floating pile groups. Geotechnique 1988;38(4):557–74.

[16] Gazetas G, Makris N. Dynamic pile–soil–pile interaction, Part I: Analysis of axial vibration. Earthq Eng Struct Dyn 1991;20(2):115–32.

[17] Makris N, Gazetas G. Dynamic pile–soil–pile interaction, Part II: Lateral and seismic respons. Earthq Eng Struct Dyn 1992;21(2):145–62.

[18] Nozoe H. Simple quasi-dynamic method for impedances of pile group foundation. J Struct Construct Eng 1999(525):49–56.

[19] Varun, Assimaki D, Gazetas G. A simplified model for lateral response of large diameter caisson foundations, linear elastic formulation. Soil Dyn Earthq Eng 2009;29(2):268–91.

[20] Varun, Assimaki D. A generalized hysteresis model for biaxial response of pile foundations in cohesionless soils. Soil Dyn Earthq Eng 2012;32(1):56–70.

[21] Varun, Assimaki D, Shafieezadeh A. Soil–pile–structure interaction simulations in liquefiable soils via dynamic macroelements: formulation and validation. Soil Dyn Earthq Eng 2013;47:92–107.

[22] Asega H, Arai T, Akira K, Suzumura J, Hanada K, Shiojuri H, et al. A dynamic response analytical method of soil pile system using dynamic interaction spring. J Struct Construct Eng 1999(526):45–52.

[23] Nogami T. Flexural response of grouped piles under dynamic loading. Earthq Eng Struct Dyn 1985;13(3):321–36.

[24] Lysmer J, Tabatabaie RM, Tajirian F, Vahdani S, Ostadan F. SASSI – a system for analysis of soil–structure interaction. Berkeley (CA): University of California; 1981. Report No.: UCB/GT/81-02.

[25] Waas G. Analysis method for footing vibrations through layered media. Berkeley (CA): University of California; 1972. Report No.: S-71-14.

[26] Shimizu N, Yamamoto S, Koori Y. Three-dimensional dynamic analysis of soil structure system by thin layer element method, Part1. Outline of analysis method and foundation of layered zone. Trans AIJ 1977;253:31–43.

[27] Kausel E. An explicit solution for the green function for dynamic loads in layered media. Massachusetts: Department of Civil Eng, M.I.T.; 1981. Report No.: R81-13.

[28] Hull S. Dynamic loads in layered halfspaces. Doctoral thesis, Massachusetts Institute of Technology; 1985.

[29] Hull S, Kausel E. Dynamic loads in layered halfspace. In: Proceedings of 5th ASCE EMD specialty conference, Laramie, Wyoming; 1984. p. 201–4.

[30] Kaynia AM, Kausel E. Dynamic behavior of pile groups. In: Proceedings of 2nd inter. conf. numer. meth. offshore piling, Austin, Texas; 1982.

[31] Architectural Institute of Japan. An introduction to dynamic soil–structure interaction. Tokyo: Gihodoshppan; 1996. 172 p.